Using Two Receiving Coils to Achieve Constant Output Power for Wireless Power Transfer

Suqi Liu* **and Yuping Liu**

Abstract—Magnetic coupling resonance wireless power transfer (MCR-WPT) technology has been in development for over a decade. The output power of the MCR-WPT system achieves the maximum value at two splitting frequencies and not at the natural resonant frequency because frequency splitting occurs in the over-coupled region. In order to achieve excellent transfer characteristics, optimization approaches have been used in many MCR-WPT projects. However, it remains a challenge to obtain a constant output power in a fixed-frequency mode. In this research, two receiving coils are used in the MCR-WPT system to achieve a uniform magnetic field. First, a circuit model of the MCR-WPT system is established, and transfer characteristics of the system are investigated by applying the circuit theory. Second, the use of two receiving coils to achieve a uniform magnetic field is investigated. Constant output power is then achieved in a fixed-frequency mode. Lastly, the experimental circuit of the MCR-WPT system is designed. The experimental results are consistent with the theoretical ones. The topology of using two receiving coils results in optimum transmission performance. Constant output power and high transfer efficiency are achieved in the higher frequency mode. If the distance between the two receiving coils is appropriate and the transmitting coil moves between the two receiving coils, the fluctuation of the output power of the MCR-WPT system is less than 10%.

1. INTRODUCTION

One hundred years ago, Nikola Tesla [1] demonstrated the principles of wireless power transfer in an experiment. Subsequently, considerable progress has been made in the field of wireless power transfer. Wireless power transfer technologies fall into two categories, i.e., non-radiative and radiative [2]. In near field or non-radiative techniques, power is transferred over mid-range distances by magnetic fields using magnetic coupling resonance between wire coils [3]; the power is transferred over short distances by magnetic fields using inductive coupling between coils; or by electric fields using capacitive coupling between metal electrodes [4]. In far-field or radiative techniques, also called power beaming, power is transferred by beams of electromagnetic radiation, such as microwaves or laser beams. These methods are used to transport energy over longer distances, but the radiation must be aimed at the receiver. Proposed applications for this type are solar powered satellites and wirelessly powered drone aircraft [5].

Magnetic coupling resonance wireless power transfer (MCR-WPT) technology was developed in 2007 [3, 6], and it is currently a popular research topics. Nowadays, MCR-WPT technology is the most widely used wireless technology; its applications include rechargeable handheld devices such as phones, electric toothbrushes; rechargeable implantable medical devices such as artificial cardiac pacemakers; and electric vehicles [7, 8].

In the over-coupled region, frequency splitting is a physical phenomenon that occurs in MCR-WPT systems [9, 10]. Thus, the output power of the two-coil MCR-WPT system achieves the maximum output

power at two splitting angular frequencies, but not at the resonant angular frequency. In contrast, the transfer efficiency of the two-coil MCR-WPT system achieves the maximum value at the resonant angular frequency but not at the two splitting angular frequencies. In addition, the vibration of the receiver coil (or relay coil) is a common phenomenon in a three-coil MCR-WPT system [11, 12]. Thus, the peaks of the output power of the transmitter and receiver coils exhibit periodic variation; the transmission efficiency of the receiver coil exhibits periodic fluctuation; and the transmission efficiency of the transmitter coil exhibits periodic variation. Because MCR-WPT exhibits these phenomena, it is rather sensitive to alignment and distance changes between the coils. Any change in the coil position from the initial optimal location results in degraded transfer performance [13]. It is well known that the output power and transfer efficiency of the MCR-WPT system are maximized when optimal impedance matching conditions exist [14, 15]. In [16], it was shown that uncertainty with regard to moving objects is a common occurrence in MCR-WPT systems. To enhance the robustness of the two-coil MCR-WPT system to uncertain parameter variations, a modified MCR-WPT system structure and an interval-based uncertain optimization method have been proposed; however, two tuning and impedance matching circuits were used to compensate for the reactive power in the MCR-WPT system. The optimization method is relatively complex. To improve the two resonant coil system, a three-coil MCR-WPT system can be used; in this system the intermediate resonant coil system with the same resonant frequency between the transmitting and receiving resonant coils extends the distance of power delivery and increases the power transfer efficiency [17, 18]. In [19], the conjugate power of the compensator loop was created via magnetic coupling of the two compensating coils that were inserted into the transmitter loop. The mechanism for dynamic impedance compensation for MCR-WPT was then provided by developing a virtual three-coil MCR-WPT system. Impedance compensation was used to adjust the magnetic field of the MCR-WPT system and the reactive power and active power of the MCR-WPT system. However, it was difficult to utilize this topology in an application because the coupled distance between the two compensating coils had to be adjusted manually. In [20], a dynamic impedance compensation for MCR-WPT was proposed by utilizing a compensator in a three-coil MCR-WPT system, and maximum output power and transfer efficiency was achieved simultaneously in the fixed-frequency mode. The scheme of dynamic compensation of the MCR-WPT using a compensator is convenient to obtain dynamic impedance compensation by adding or removing capacitances or inductances from the compensator. However, the addition or removal of capacitances or inductances from the compensator will cause a transient impact on the MCR-WPT system. Therefore, the previously proposed approaches have drawbacks in practical applications.

Based on the above-mentioned studies and drawbacks, we propose an improvement of the MCR-WPT system and present a topology of a three-coil MCR-WPT system that includes two receiving coils. This study focuses on how to use two receiving coils to achieve a uniform magnetic field. Constant output power is then achieved in a fixed-frequency mode under a variety of operating conditions. First, the circuit model of the MCR-WPT system, which includes two receiving coils, is established, and the transfer characteristics are described. Second, the output power and transfer efficiency are analyzed and simulated using the Biot-Savart law [21] and simulation software. Lastly, the experimental circuit of the MCR-WPT system is described. The experimental results are consistent with the theoretical ones. The topology using two receiving coils results in optimizing the transmission performance; constant output power and high transfer efficiency are achieved in the higher frequency mode.

2. MODELING OF THE MCR-WPT SYSTEM WITH TWO RECEIVING COILS

Figure 1 shows the diagram of the MCR-WPT system with the two receiving coils. This topology results in constant output power and high transfer efficiency. Figure 1(a) shows a sketch of the MCR-WPT system that includes two receiving coils L_2 and L_3. The equivalent circuit of the MCR-WPT system includes two receiving coils L_2 and L_3, as shown in Figure 1(b).

The circuit model consists of two resonant circuits. U_S is the input power of the transmitter. R_1 and R_2 are the resistances of the coils. L_1, L_2, and L_3 are the inductances. C_1 and C_2 are the capacitances. R_L is the load resistance. d_1 is the coupling distance between L_1 and L_2 coils. d_2 is the coupling distance between L_1 and L_3 coils. $d_3 = d_1 + d_2$ is the coupling distance between L_2 and L_3 coils. M_1 is the mutual inductance of L_1 and L_2 coils. M_2 is the mutual inductance of L_1 and L_3 coils.
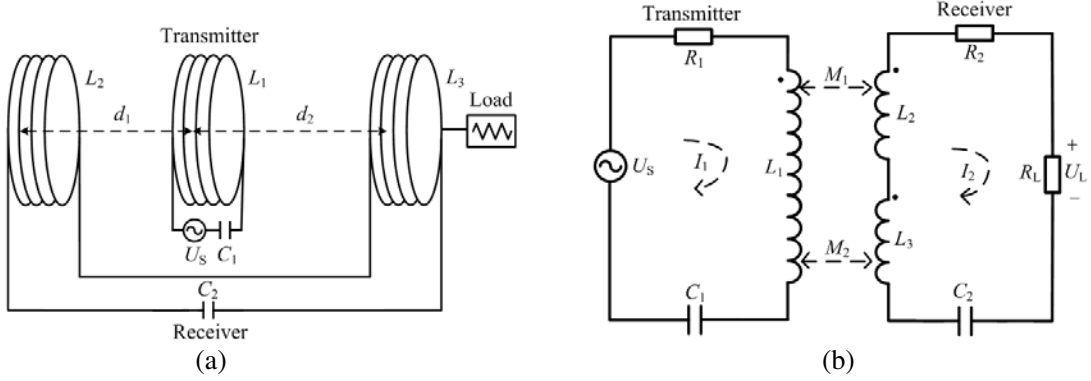
Figure 1. Model of the MCR-WPT system that includes two receiving coils to achieve a uniform magnetic field and then to achieve constant output power and high transfer efficiency. (a) Sketch of the MCR-WPT system with two receiving coils L_2 and L_3. (b) Equivalent circuit of the MCR-WPT system with two receiving coils L_2 and L_3.

For the convenience of analysis, the mutual inductance of L_2 and L_3 coils is ignored because M_1 and M_2 are much larger.

The equivalent circuit model provides a convenient reference for the analysis of the transfer characteristics of the MCR-WPT system. For simplicity, the assumed parameters of the transmitter and receiver are listed in Table 1.

Table 1. Assumed values for the individual circuit elements of the transmitter and receiver.

Parameter	Value
Capacitances of the transmitter and receiver	$C_1 = 2C_2 = C$
Inductances of the transmitter and receiver	$L_1 = L_2 = L_3 = L$
Resistance of the receiver	$R_2 + R_L = 2R$
Resistance of the transmitter	$R_1 = \sigma R$
Ratio of resistance of the load	$R_L = \beta R$
Resonance angular frequency of the system	$\omega_0 = 1/(LC)^{0.5}$
Resonance frequency of the system	$f_0 = \omega_0/2\pi$
Quality factor of the system	$Q_0 = \omega_0 L/R = 1/(\omega_0 CR)$
Frequency detuning factor of the system	$\xi = Q_0(\omega/\omega_0 - \omega_0/\omega)$
Resonance angular frequency of the transmitter and receiver	ω_0
Quality factor of the transmitter	$Q_1 = \omega_0 L_1/R_1 = 1/(\omega_0 C_1 R_1) = Q_0/\sigma$
Quality factor of the receiver	$Q_2 = \omega_0(L_2+L_3)(R_2+R_L) = 1/(\omega_0 C_2(R_2+R_L)) = Q_0$

Figure 1(b) shows the MCR-WPT system with a driving source of angular frequency ω, where Kirchhoff's voltage law is applied to determine the currents in each resonant circuit as shown in Equation (1), where the self-impedance of transmitter Z_1 and receiver Z_2 is expressed as Equation (2) [19, 20].

$$\begin{cases} Z_1 I_1 - j\omega M_1 I_2 - j\omega M_2 I_2 = U_S \\ Z_2 I_2 - j\omega M_1 I_1 - j\omega M_2 I_1 = 0 \end{cases} \tag{1}$$

$$\begin{cases} Z_1 = R_1 + j\omega L_1 + \dfrac{1}{j\omega C_1} = \left(\sigma + \dfrac{j\omega_0 L}{R}\dfrac{\omega}{\omega_0} + \dfrac{1}{j\omega_0 CR}\dfrac{\omega_0}{\omega}\right) R = (\sigma + j\xi)R \\ Z_2 = R_2 + R_L + j\omega(L_2 + L_3) + \dfrac{1}{j\omega C_2} = \left(2 + 2\dfrac{j\omega_0 L}{R}\dfrac{\omega}{\omega_0} + 2\dfrac{1}{j\omega_0 CR}\dfrac{\omega_0}{\omega}\right) R = 2(1 + j\xi)R \end{cases} \tag{2}$$

According to [19], Z_{11} and Z_{22} represent the self-impedance; $(\omega M)^2/Z_{11}$ and $(\omega M)^2/Z_{22}$ represent the reflecting impedances. In order to consider the coupled effects of the resistance of the resonances and simplify Equation (4), impedance coupling factors τ_1 and τ_2 are defined as in Equation (3), which indicates the ability of the impedance coupling, where R_S is the resistance of U_S, $Z_{11} = R_1 + R_S + j\omega L_1 + (j\omega C_1)^{-1}$, $Z_{22} = R_2 + R_L + j\omega L_2 + (j\omega C_2)^{-1}$, and M is the mutual inductance of the transmitter and receiver coils in the two-coil MCR-WPT system.

$$\begin{cases} \tau_1 = \dfrac{\omega M_1}{\sqrt{R_1(R_2 + R_L)}} = \dfrac{\omega M_1}{\sqrt{2\sigma}R}, \tau_1 > 0 \\ \tau_2 = \dfrac{\omega M_2}{\sqrt{R_1(R_2 + R_L)}} = \dfrac{\omega M_2}{\sqrt{2\sigma}R}, \tau_2 > 0 \end{cases} \tag{3}$$

According to Equations (1), (2), and (3), as well as the definitions in Table 1, the currents of the transmitter and receiver coils can be written as

$$\begin{cases} I_1 = \dfrac{1 + \xi^2}{\sigma\left[1 + (\tau_1 + \tau_2)^2 + \xi^2\right] + j\xi[1 + \xi^2 - \sigma(\tau_1 + \tau_2)^2]} \dfrac{U_S}{R} \\ I_2 = \dfrac{\sqrt{\sigma/2}(\tau_1 + \tau_2)(\xi + j)}{\sigma\left[1 + (\tau_1 + \tau_2)^2 + \xi^2\right] + j\xi\left[1 + \xi^2 - \sigma(\tau_1 + \tau_2)^2\right]} \dfrac{U_S}{R} \end{cases} \tag{4}$$

According to the root mean square (RMS) current I_2 of the receiver coil, the power transferred to the load resistance (the output power of the MCR-WPT system) is $P_{out} = |I_2|^2 R_L$. Let $\partial P_{out}/\partial \xi = 0$, and we obtain three roots: $\xi_1 = 0$, $\xi_2 = -[\sigma(\tau_1 + \tau_2)^2 - 1]^{0.5}$, and $\xi_3 = [\sigma(\tau_1 + \tau_2)^2 - 1]^{0.5}$. If $\xi = 0$, $\tau_1 + \tau_2 = 1$, the output power of the system achieves the maximum value $P_{\text{outmax}} = (\beta U_S^2)/(8\sigma R)$. Thus, the normalized output power of the system is

$$\psi = \frac{P_{out}}{P_{out\,\max}} = \frac{4\sigma^2(\tau_1 + \tau_2)^2(1 + \xi^2)}{\sigma^2[1 + (\tau_1 + \tau_2)^2 + \xi^2]^2 + \xi^2[1 + \xi^2 - \sigma(\tau_1 + \tau_2)^2]^2} \tag{5}$$

The input power of the MCR-WPT system is $P_{in} = |I_1|^2 R_1 + |I_2|^2(R_2 + R_L)$. Thus, the transfer efficiency of the MCR-WPT system can be written as

$$\eta = \frac{P_{out}}{P_{in}} = \frac{|I_2|^2 R_L}{|I_1|^2 R_1 + |I_2|^2(R_2 + R_L)} = \frac{\beta(\tau_1 + \tau_2)^2}{2(1 + \xi^2) + (\tau_1 + \tau_2)^2} \tag{6}$$

3. SIMULATION ANALYSIS OF THE MCR-WPT SYSTEM

In physics, the Biot-Savart law relates the magnetic field to the magnitude, direction, length, and proximity of the electric current. The law is valid in the magnetostatic approximation and is consistent with both Ampere's circuital law and Gauss's law for magnetism [21]. Figure 2 shows a sketch of the mutual inductance of the MCR-WPT system with two receiving coils, which achieves a uniform magnetic field and then achieves constant output power and high transfer efficiency under a variety of operating conditions. According to the Biot-Savart law, the induction intensity of the circular coil L_1 at the position of coil L_2 equals B_1; the induction intensity of the circular coil L_1 at the position of coil L_3 equals B_2. Thus, B_1 and B_2 can be written as

$$\begin{cases} B_1 = \dfrac{\mu_0(n_1 n_2)^{0.5} r_1^2 I_1}{2(r_1^2 + d_1^2)^{3/2}} \\ B_2 = \dfrac{\mu_0(n_1 n_3)^{0.5} r_1^2 I_1}{2(r_1^2 + d_2^2)^{3/2}} \end{cases} \tag{7}$$

where $\mu_0 = 4\pi \times 10^{-7}$ H/m is the permeability of vacuum; r_1, r_2, and r_3 are radii of the Tx, M-Rx, and S-Rx coils, respectively; n_1, n_2, and n_3 are the turn numbers of the Tx, M-Rx, and S-Rx coils, respectively; O is the central point between M-Rx and S-Rx coils; O_1, O_2, and O_3 are the geometric centers of the Tx, M-Rx, and S-Rx coils, respectively; x is the distance between the points O_1 and O; this is a variable value.
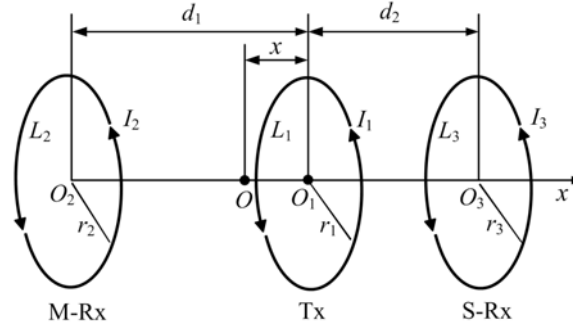
Figure 2. Sketch of the mutual inductance of the MCR-WPT system with two receiving coils that achieves a uniform magnetic field and then achieves constant output power and high transfer efficiency. The sketch includes the transmitter coil (Tx) L_1, main receiver coil (M-Rx) L_2, and sub-receiver coil (S-Rx) L_3.

According to Equation (7) and Figure 1, mutual inductances M_1 and M_2 are

$$\begin{cases} M_1 = \dfrac{\Phi_1}{I_1} = \dfrac{\pi r_2^2 B_1}{I_1} = \dfrac{\pi \mu_0 (n_1 n_2)^{0.5} (r_1 r_2)^2}{2(r_1^2 + d_1^2)^{3/2}} \\[4mm] M_2 = \dfrac{\Phi_2}{I_1} = \dfrac{\pi r_3^2 B_2}{I_1} = \dfrac{\pi \mu_0 (n_1 n_3)^{0.5} (r_1 r_3)^2}{2(r_1^2 + d_2^2)^{3/2}} \end{cases} \tag{8}$$

where Φ_1 represents the magnetic flux of the magnetic field excited by coil L_1 through coil L_2; Φ_2 represents the magnetic flux of the magnetic field excited by coil L_1 through coil L_3.

According to Equations (3) and (8), the impedance coupling factors τ_1 and τ_2 in Equation (3) can also be written as

$$\begin{cases} \tau_1 = \dfrac{\pi \omega \mu_0 (n_1 n_2)^{0.5} (r_1 r_2)^2}{2\sqrt{2\sigma} R \left(r_1^2 + d_1^2\right)^{3/2}} = \dfrac{\pi \omega \mu_0 (n_1 n_2)^{0.5} (r_1 r_2)^2}{2\sqrt{2\sigma} R \left(r_1^2 + \left(\dfrac{d_1 + d_2}{2} + x\right)^2\right)^{3/2}} \\[6mm] \tau_2 = \dfrac{\pi \omega \mu_0 (n_1 n_3)^{0.5} (r_1 r_3)^2}{2\sqrt{2\sigma} R (r_1^2 + d_2^2)^{3/2}} = \dfrac{\pi \omega \mu_0 (n_1 n_3)^{0.5} (r_1 r_3)^2}{2\sqrt{2\sigma} R \left(r_1^2 + \left(\dfrac{d_1 + d_2}{2} - x\right)^2\right)^{3/2}} \end{cases} \tag{9}$$

As shown in Figures 1 and 2, we assume that the coupling distance between the main receiver and sub-receiver coils $d_3 = d_1 + d_2$ equals 24 mm. Using Equations (5) and (6), the impedance coupling factors τ_1 and τ_2 written in Equation (9), as well as the simulation parameters in Table 2, MATLAB software was used to determine the output power and transfer efficiency of the MCR-WPT system; the results are plotted in Figure 3.

In Figure 3(a), the output power between O_1 and O_3 should be superimposed in the series mode because the main receiver and sub-receiver coils are connected in series. It is evident that the output power of $\tau_1 + \tau_2$ curve is the sum of the output power of τ_1 curve and output power of τ_2 curve. However, the transfer efficiency of the $\tau_1 + \tau_2$ curve does not equal the sum of the transfer efficiency of τ_1 curve and transfer efficiency of τ_2 curve. Thus, this simulation and the following experiments once again prove that the MCR-WPT system is a power superposition system [19]. Between points O_1 and O_3, the output power and transfer efficiency almost achieve constant values because the two receiving coils achieve uniform magnetic field [22]. Outside of points O_1 and O_3, the output power and transfer efficiency of the system decrease significantly. Thus, the two receiving coils used in this study achieve a uniform magnetic field and then achieves constant output power and high transfer efficiency between the main receiver and sub-receiver coils. Next, we will verify these simulation results in detail using experiments.

Table 2. Simulation parameters of the output power and transfer efficiency of the MCR-WPT system.

Parameter	Tx	M-Rx	S-Rx
Frequency f_0/kHz	140	140	140
Inductance L/µH	29.25	29.25	29.25
Capacitance C/nF	44.18	22.09	
Radius r/m	23×10^{-3}	23×10^{-3}	23×10^{-3}
Number of turns n	20	20	20
Distance $d_3 = d_1 + d_2$/m		24×10^{-3}	
Impedance scaling factor σ		1	
Frequency detuning factor ξ		0	
Load R_L/Ω			0.5
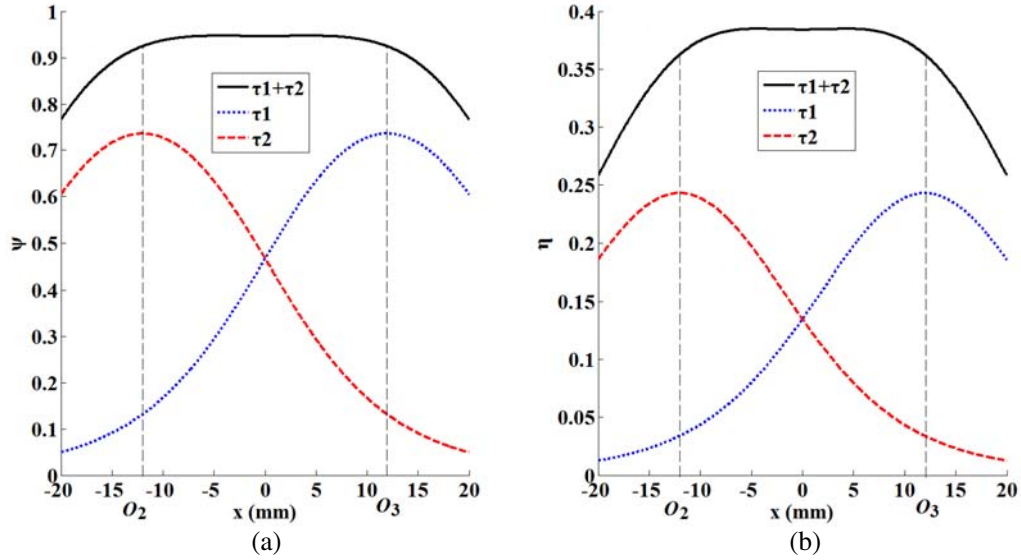
Figure 3. Characteristic curves of the output power and transfer efficiency of the MCR-WPT system with two receiving coils. (a) Characteristic curves of the output power of the MCR-WPT system. (b) Characteristic curves of the transfer efficiency of the MCR-WPT.

4. EXPERIMENTAL RESULTS OF THE MCR-WPT SYSTEM

Figure 4 shows the topology of using two receiving coils to achieve a uniform magnetic field and then to achieve constant output power and high transfer efficiency under a variety of operating conditions in a fixed-frequency mode. The MCR-WPT experimental system includes the power amplifier, wave generator, oscilloscope, voltage probes, capacitances, transmitter, receiver, load, transmitting coil, and receiving coils. The main parameters of the transmitter and receiver are listed in Table 2. The experiment includes two steps to ascertain the transfer characteristics of the output power and transfer efficiency. (a) The transfer characteristics of the output power and transfer efficiency are determined at different frequencies. This allows us to determine the optimal driving source frequency to achieve the maximum output power or maximum transfer efficiency of the system. (b) When the system operates at the optimal driving source frequency, transfer characteristics of the output power, and transfer efficiency for the variable x will be revealed.

In the experiments, we ensured that the coupling distance d_3 was constant and that the values were

20 mm, 30 mm, and 36 mm; the variable x was zero; subsequently, the voltages and currents of the input and output were measured by using the voltage and current probes at the different frequencies. Figures 5 and 6 show the results of the experiments. At a coupling distance d_3 equal to 20 mm, the output power of the system exhibits two peaks, i.e., one at the frequency of 100 kHz and the other at the frequency of 140 kHz. When the coupling distance d_3 equals 30 mm, the two peaks occur at the frequencies of 105 kHz and 135 kHz. At a coupling distance between the main receiver and the sub-receiver coils d_3 equal to 36 mm, and the two peaks occur at the frequencies of 105 kHz and 135 kHz (Figure 5). At the coupling distances between the main receiver and sub-receiver coils d_3 of 20 mm, 30 mm, and 36 mm, the system achieves the maximum transfer efficiency at the frequency of 135 kHz (Figure 6). We use the resonance frequency of the system ($f_0 = 120$ kHz) as a demarcation point. Thus, the frequencies of 100 kHz and 105 kHz belong to the lower frequency mode, and the frequencies of 135 kHz and 140 kHz belong to the higher frequency mode.

The experimental results show that the MCR-WPT system achieves maximum output power in the lower frequency mode or higher frequency mode. However, because the system is affected by the mutual inductance of L_2 and L_3 coils, the MCR-WPT system achieves the maximum transfer efficiency in the higher frequency mode [19, 20]. For a comparative analysis, the resonance frequency of the system ($f_0 = 120$ kHz) was also included in the subsequent experiments. These frequencies were used (i.e., 100 kHz, 105 kHz, 120 kHz, 135 kHz, and 140 kHz), and they remained fixed. The coupling distance of the main receiver and sub-receiver coils d_3 (20 mm, 30 mm, and 36 mm) was constant, and the voltages
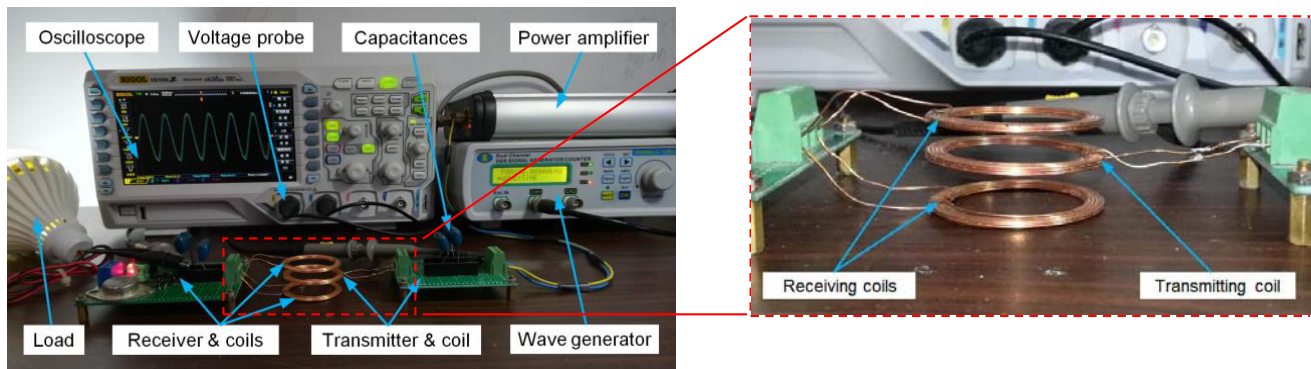

Figure 4. Experimental system of using two receiving coils to achieve a uniform magnetic field and then to achieve the constant output power and high transfer efficiency.
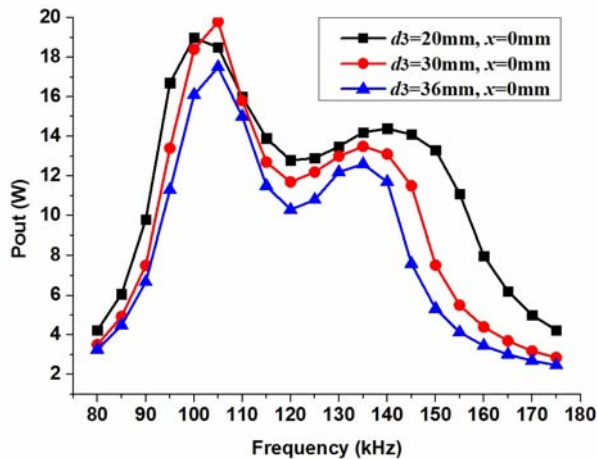

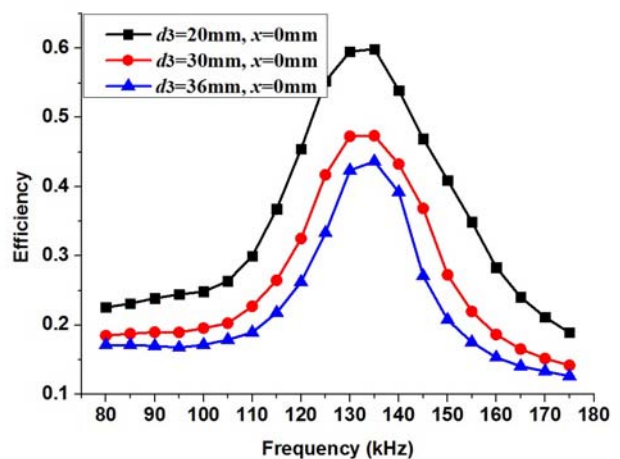**Figure 5.** Output power of the system for different frequencies.

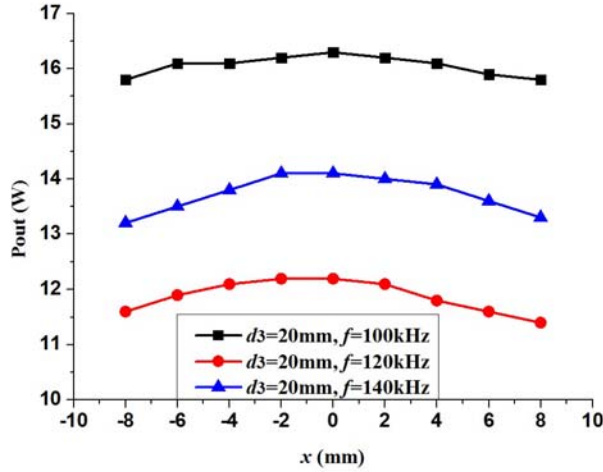**Figure 6.** Transfer efficiency of the system for different frequencies.

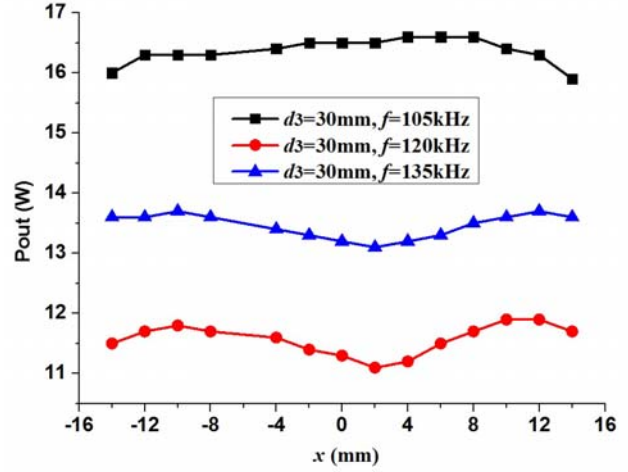**Figure 7.** Output power for variable x when $d_3 = 20$ mm.

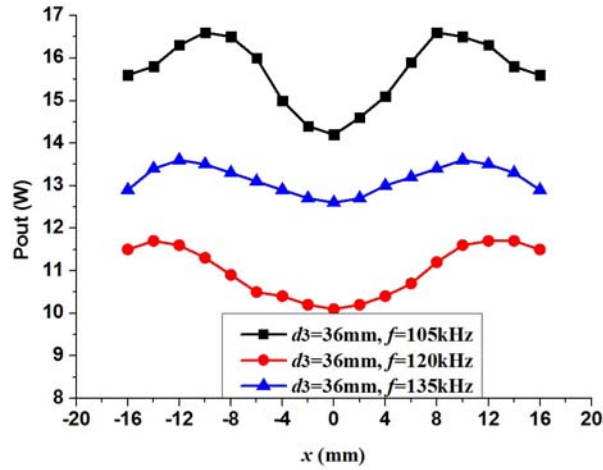**Figure 8.** Output power for variable x when $d_3 = 30$ mm.

Figure 9. Output power for variable x when $d_3 = 36$ mm.
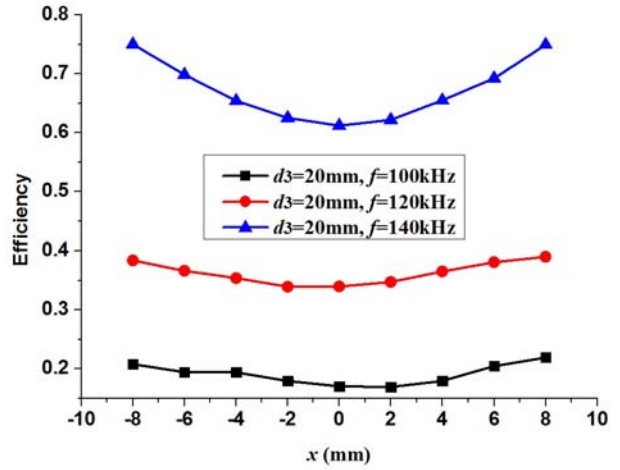

Figure 10. Transfer efficiency for variable x when $d_3 = 20$ mm.

and currents of the input and output were measured for variable x. Figures 7, 8, 9, 10, 11, and 12 show the results of these experiments.

In Figures 7, 8, and 9, at the center between the receiving coils, the output power increases from the minimum value to maximum value as distance d_3 decreases because the MCR-WPT system is a power superposition system [19]. In Figures 7, 8, it is observed that the MCR-WPT system almost achieves constant output power regardless of whether the system is in the lower frequency mode, resonance frequency point, or higher frequency mode; the fluctuation of the output power is less than 10%. The MCR-WPT system obtains the minimum output power at $x = 0$ by power superposition because distance d_3 is large (Figure 9).

As shown in Figures 10, 11, and 12, the transfer efficiency first decreases and then increases as the variable x increases. In the higher frequency mode (namely, $f = 135$ kHz or 140 kHz), the transfer efficiency of the system achieves a higher value. The system achieves constant transfer efficiency as distance d_3 decreases. However, in the lower frequency mode or resonance frequency point (namely, $f = 100$ kHz, 105 kHz, or 120 kHz), the transfer efficiency of the system obtains a lower value.

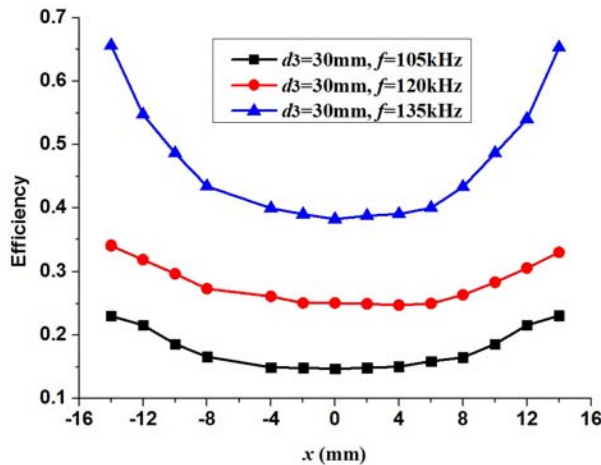In summary, the experimental results are consistent with the simulated ones. In the higher

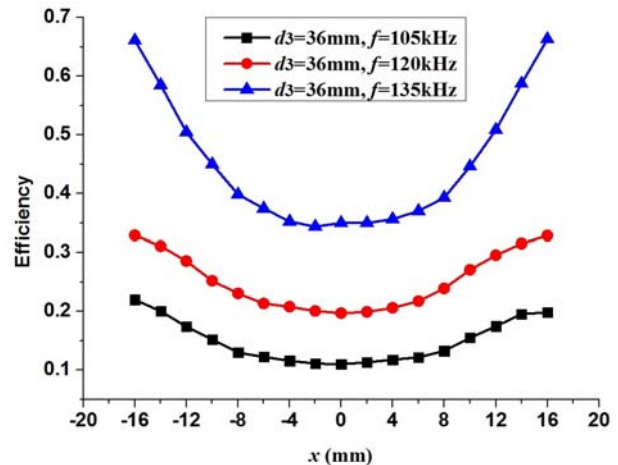**Figure 11.** Transfer efficiency for variable x when $d_3 = 30$ mm.

Figure 12. Transfer efficiency for variable x when $d_3 = 36$ mm.

frequency mode, when the coupling distance d_3 between the main receiver and sub-receiver coils is constant and the variable x changes, the system achieves constant output power and high transfer efficiency in the fixed-frequency mode because two receiving coils are used to achieve a uniform magnetic field.

5. DISCUSSION

When a transmitting coil is placed between two receiving coils, there are space limits. Namely, the transmitting coil only moves between two receiving coils. However, in some specific applications, this topology may provide a practical solution. In any case, using two receiving coils to achieve a uniform magnetic field and then to achieve the constant output power of the MCR-WPT system is a good idea. The results of this study may help researchers to find an approach that achieves constant output power and transfer efficiency in open areas, such as charging pads. We believe that this study will accelerate practical adaptations of wireless power transfer.

6. CONCLUSION

In this study, an efficient topology was proposed for an MCR-WPT system with two receiving coils. The transfer characteristics of the MCR-WPT system were analyzed using the Biot-Savart law, and simulations were conducted using MATLAB software. The results of the experiment were consistent with the simulation. Two receiving coils were used to achieve a uniform magnetic field. In the higher frequency mode, when the distance between the two receiver coils was appropriate, constant output power and high transfer efficiency were achieved in the fixed-frequency mode under a variety of operating conditions. Overall, the results of this study demonstrate that the topology of using two receiving coils results in optimum transmission performance.

ACKNOWLEDGMENT

REFERENCES

1. Tesla, N., "Electrical energy," U.S. Patent 1,119,732, Dec. 1, 1914.

2. Wireless power transfer, https://en.wikipedia.org/wiki/Wireless_power_transfer.

3. Kurs, A., A. Karalis, R. Moffatt, et al., "Wireless power transfer via strongly coupled magnetic resonances," *Science*, Vol. 317, No. 5834, 83, 2007

4. Erfani, R., F. Marefat, A. M. Sodagar, et al., "Modeling and characterization of capacitive elements with tissue as dielectric material for wireless powering of neural implants," *IEEE Transactions on Neural Systems and Rehabilitation Engineering*, Vol. 26, No. 5, 1093, 2018.

5. Mcspadden, J. O. and J. C. Mankins, "Space solar power programs and microwave wireless power transmission technology," *IEEE Microwave Magazine*, Vol. 3, No. 4, 46, 2002.

6. Karalis, A., J. D. Joannopoulos, and M. Soljačić, "Efficient wireless non-radiative mid-range energy transfer," *Annals of Physics*, Vol. 323, No. 1, 34, 2006.

7. Liu, Y., B. Li, M. Huang, et al., "An overview of regulation topologies in resonant wireless power transfer systems for consumer electronics or bio-implants," *Energies*, Vol. 11, No. 7, 1737, 2018.

8. Lu, F., H. Zhang, and C. Mi, "A two-plate capacitive wireless power transfer system for electric vehicle charging applications," *IEEE Transactions on Power Electronics*, Vol. 33, No. 2, 964, 2018.

9. Sample, A. P., D. T. Meyer, and J. R. Smith, "Analysis, experimental results, and range adaptation of magnetically coupled resonators for wireless power transfer," *IEEE Transactions on Industrial Electronics*, Vol. 58, No. 2, 544, 2011.

10. Zhang, Y., Z. Zhao, and K. Chen, "Frequency-splitting analysis of four-coil resonant wireless power transfer," *IEEE Transactions on Industry Applications*, Vol. 50, No. 4, 2436, 2014.

11. Liu, S., J. Tan, and X. Wen, "Modeling of coupling mechanism of wireless power transfer system and vibration phenomenon of receiver-coil in three-coil system," *AIP Advances*, Vol. 7, 115107, 2017.

12. Liu, S. and J. Tan, "Study on the vibration mechanism of the relay coil in a three-coil WPT system," *Progress In Electromagnetics Research M*, Vol. 70, 117, 2018

13. Huang, R., B. Zhang, D. Qiu, et al., "Frequency splitting phenomena of magnetic resonant coupling wireless power transfer," *IEEE Transactions on Magnetics*, Vol. 50, No. 11, 1, 2014.

14. Duong, T. P. and J. W. Lee, "A dynamically adaptable impedance-matching system for midrange wireless power transfer with misalignment," *Energies*, Vol. 8, No. 8, 7593, 2015.

15. Xiao, C., "New insight of maximum transferred power by matching capacitance of a wireless power transfer system," *Energies*, Vol. 10, No. 5, 688, 2017.

16. Luo, Y., Y. Yang, X. Wen, et al., "Enhancing the robustness of the wireless power transfer system to uncertain parameter variations using an interval-based uncertain optimization method," *Energies*, Vol. 11, No. 8, 2032, 2018.

17. Kim, J., H.-C. Son, K.-H. Kim, et al., "Efficiency analysis of magnetic resonance wireless power transfer with intermediate resonant coil," *IEEE Antennas Wireless Propagation Letters*, Vol. 10, 389, 2011.

18. Zhang, F., S. A. Hackworth, W. Fu, et al., "Relay effect of wireless power transfer using strongly coupled magnetic resonances," *IEEE Transactions on Magnetics*, Vol. 47, No. 5, 1478, 2011.

19. Liu, S., J. Tan, and X. Wen, "Dynamic impedance compensation for wireless power transfer using conjugate power," *AIP Advances*, Vol. 8, 025210, 2018.

20. Liu, S. and J. Tan, "Dynamic impedance compensation for WPT using a compensator in a three-coil wireless power transfer system," *Circuit World*, Vol. 44, No. 4, 171, 2018.

21. Biot-Savart law, https://en.wikipedia.org/wiki/Biot%E2%80%93Savart_law.

22. Helmholtz coil, https://en.wikipedia.org/wiki/Helmholtz_coil.